Modeling thermodynamic properties of propane or tetrahydrofuran mixed with carbon dioxide or methane in structure-II clathrate hydrates

Fang, Bin; Ning, Fulong; Cao, Pinqiang; Peng, Li; Wu, Jianyang; Zhang, Zhun; Vlugt, Thijs J.H.; Kjelstrup, Signe

DOI
10.1021/acs.jpcc.7b06623

Publication date
2017

Document Version
Accepted author manuscript

Published in
The Journal of Physical Chemistry C

Citation (APA)
Fang, B., Ning, F., Cao, P., Peng, L., Wu, J., Zhang, Z., Vlugt, T. J. H., & Kjelstrup, S. (2017). Modeling thermodynamic properties of propane or tetrahydrofuran mixed with carbon dioxide or methane in structure-II clathrate hydrates. *The Journal of Physical Chemistry C*, *121*(43), 23911–23925. https://doi.org/10.1021/acs.jpcc.7b06623

Modeling Thermodynamic Properties of Propane or Tetrahydrofuran Mixed with Carbon Dioxide or Methane in Structure-II Clathrate Hydrates

Bin Fang[1], Fulong Ning[1,2]*, Pinqiang Cao[1], Li Peng[1], Jianyang Wu[3], Zhun Zhang[1], Thijs J.H. Vlugt [4], Signe Kjelstrup[5]

1 Faculty of Engineering, China University of Geosciences, Wuhan, Hubei 430074, China.
2 Laboratory for Marine Mineral Resources, Qingdao National Laboratory for Marine Science and Technology, Qingdao 266237, China
3 Department of Physics, Research Institute for Biomimetics and Soft Matter, Fujian Provincial Key Laboratory for Soft Functional Materials Research, Xiamen University, Xiamen 361005, China
4 Process and Energy Department, Delft University of Technology, Leeghwaterstraat 39, 2628CB Delft, The Netherlands
5 PoreLab, Department of Chemistry, Norwegian University of Science and Technology (NTNU), Trondheim N-7491, Norway

Email address: fangbin126@cug.edu.cn

Pinqiang@cug.edu.cn

lp054101@163.com

jianyang@xmu.edu.cn

zhangz162478@cug.edu.cn

t.j.h.vlugt@tudelft.nl

signe.kjelstrup@ntnu.no

*To whom correspondence should be addressed: nflzx@cug.edu.cn

Abstract

A sound knowledge of thermodynamic properties of sII hydrates is of great importance to understand the stability of sII gas hydrates in petroleum pipelines and in natural settings. Here, we report direct molecular dynamics (MD) simulations of the thermal expansion coefficient, the compressibility and the specific heat capacity of C_3H_8, or tetrahydrofuran (THF), in mixtures of CH_4 or CO_2, in sII hydrates under a wide, relevant range of pressure- and temperature conditions. The simulations were started with guest molecules positioned at the cage center of the hydrate. Annealing simulations were additionally performed for hydrates with THF. For the isobaric thermal expansion coefficient, an effective correction method was used to modify the lattice parameters, and the corrected lattice parameters were subsequently used to obtain thermal expansion coefficients in good agreement with experimental measurements. The simulations indicated that the isothermal expansion coefficient and the specific heat capacity of C_3H_8 - pure hydrates were comparable, but slightly larger than those of THF- pure hydrates, which could form Bjerrum defects. The considerable variation in the compressibility between the two, appeared to be due to crystallographic defects. However, when a second guest molecule occupied the small cages of the THF hydrate, the deviation was smaller, because the subtle guest-guest interactions can offset an unfavorable configuration of unstable THF hydrates, caused by local defects in free energy. Unlike the methane molecule, the carbon dioxide molecule, when filling the small cage, can increase the expansion coefficient and compressibility as well as decrease the heat capacity of the binary hydrate, similar to the case of sI hydrates. The calculated bulk modulus for C_3H_8 pure and binary hydrates with CH_4 or CO_2 molecule varied between 8.7 and 10.6 GPa at 287.15K between 10 and 100MPa. The results for the specific heat capacities varied from 3155 to 3750.0 J kg^{-1} K^{-1} for C_3H_8 pure and binary hydrates with CH_4 or CO_2 at 287.15K. These results are the first of this kind reported so far. The simulations show that the thermodynamic properties of hydrates largely depend on the enclathrated compounds. This provides a much-needed atomistic characterization of the sII hydrate properties, and gives an essential input for large-scale discoveries of hydrates and processing as a potential energy source.

Key words: mixed propane clathrate hydrate; expansion coefficient; compressibility; heat capacity

1. Introduction

Clathrate hydrates, known as non-stoichiometric inclusion compounds, are ice-like crystal hydrates in which certain compounds (they are hydrate formers) stabilize the network formed by hydrogen-bonded concomitant water molecules.[1] If the hydrate formers exist in the state of a gas, the clathrate hydrates are called gas hydrates. Three typical hydrate structures (cubic sI, cubic sII and hexagonal sH)[2] have been identified in the permafrost region and in deep oceans as well as in pipelines[3]. A conservative assessment suggests that hydrates, when considered as potential future energy resources[4], represent twice the energy stored in all other fossil fuel deposits[5]. There are three effective recovery methods for production of CH_4 from gas hydrates deposits. Replacement of methane hydrates by CO_2 is one of those[6]. Moreover, because of the high occupancy and selectivity of clathrate hydrates, various industrial applications have been suggested, such as gas storage, seawater desalination[7-8], gas sequestration and transportation[4, 9-13]. Other significant impacts of gas hydrates relate to flow assurance[14], global climate change, the carbon cycle, ecosystems, marine geohazards, etc.

In almost all of the previously mentioned applications, the understanding of thermodynamic properties such as the thermal expansion coefficient, the isothermal compressibility and the heat capacity at constant pressure of the gas hydrates are essential. As for the thermal expansion coefficient, the basic information is critical for risk assessment studies of the mechanical stability of the earth strata hosting hydrates[15]. Seismic waves are usually employed in order to detect natural gas hydrates in sedimentary layers, and the wave speed is connected with the elastic constants and compressibility of the media through which they propagate[16]. Additionally, the heat capacity is not only used for the modelling of natural gas production from hydrate-bearing sediments, but also for hazard mitigation in conventional hydrocarbon extraction[17]. On a global scale, thermal properties provide a key for studies of climate changes related to methane release from natural hydrates[17].

Most of the thermal and mechanical properties of gas hydrates can provide insight into the properties of other compounds like ice, I_h, because of the common hydrogen-bond dominated network. While most thermodynamic properties are very similar, some of them differ widely between gas hydrates and ice I_h, such as thermal conductivity and thermal expansion coefficient. The thermal conductivity of clathrate hydrates is anomalously low as compared to that of ice I_h due to the vibrational coupling of guest gas and host water molecules[18-19] On the other hand, the thermal expansion coefficient is much larger than that of ice I_h below 200K[20]. Several studies have been done to investigate these anomalous properties of hydrates. The conclusion is that thermal conductivity and thermal expansion coefficient are related to the crystal type, guest type and size, as well as the occupancy[19-26].

Large quantities of experimental results exist for the thermal expansion coefficient[20, 27-32], compressibility[17, 33-36] or bulk modulus, and heat capacity[17, 37-39]of clathrate hydrates. Unfortunately, these experimental values are mostly available in a limited and insufficient temperature - and pressure range. In addition, to measure such properties are rather difficult, time-consuming and costly, and the results can be strongly impacted by the purity of simple[15, 40]. Molecular dynamic simulations have been shown to be a valid tool to probe the nature of gas hydrates on a molecular scale and link the microscopic behavior to macroscopic properties[7-8, 41]. There are many studies on clathrate hydrates using MD simulation to calculate thermal expansion coefficient, compressibility and heat capacity[23]. Those results were used to validate experimental reports and obtain deeper relationships between hydrates' configurations and thermodynamic properties. So far, most of studies have focused on sI hydrates[40, 42-44] with fewer studies of sII and sH hydrates[45-46]. Although the dominant structure of gas hydrates in nature is structure I (methane hydrate), sII and sH

hydrates are also common in several regions, such as the Gulf of Mexico, Cascadia Margin[47-49], and South China Sea. Davidson et al.[49] also estimated the gas component of the near-seafloor hydrates samples from the Gulf of Mexico. They carried out carbon-13 NMR and powder XRD measurements and confirmed the sII hydrate. The sII hydrates made up more than 80% of the water in the core materials (80.5 wt% water, 13.6 wt% gas and 5.9 wt% solid residue), and no sI hydrates were detected. Therefore, to understand the properties of sII hydrates is also necessary and important to understand their behavior and evolution in natural deposits.

Cubic structure II (sII) clathrate hydrate, with a unit cell denoted as $16M_S8M_L136H_2O$ has 16 small pentagonal dodecahedron cages and eight hexakaidecahedron large cages.[50] C_3H_8 and THF hydrates are two typical hydrates with sII crystalline phase, one is the major component of structure II hydrates in sediments and the other is a promising analog material for CO_2 recovery from flue gas[51] as well as for hydrogen storage[4, 10]. It was used as a prototype for all hydrates to investigate, for example, the hydrates' thermodynamics properties[52-53]. Studies have demonstrated that the guest-host hydrogen bonding in THF hydrates leads to the formation of Bjerrum defects in the THF water lattice[54-55]. This may explain the fast dielectric relaxation of hydrates[56] and the fast kinetics of stoichiometric hydrates phase formation from ice at low temperatures[57-58]. The difference in thermodynamic properties of C_3H_8 and THF hydrates can provide evidence that those properties are characteristic for the molecule involved and help comprehend the importance of guest-host interaction under similar conditions. To date, there are few studies of isobaric expansion coefficient, isothermal compressibility and heat capacity of C_3H_8 and THF hydrates by MD simulation, especially under low temperature conditions.

In addition, the small cages of sII hydrates are often occupied by relative small molecules (also called secondary "help-gases") like CH_4 and CO_2 molecules, which stabilize the structure II hydrate lattice[59-60] and affect the clathrate structure[55] in binary hydrates. For that reason, it may also be significant to know the thermodynamic properties of sII hydrates in the presence of small molecules (CH_4 and CO_2). This is relevant for the gas production process from natural gas hydrates deposits, for example, the replacement of CH_4 hydrates by CO_2 from the deposits. We shall therefore also report results of calculations of the thermal expansion coefficient, the isothermal compressibility and the specific heat capacity for the sII structure with C_3H_8, THF in the presence of CH_4 and CO_2, all using MD simulations. From this basis, we discuss effects caused by host-host, guest-host and guest-guest coupling interaction on thermodynamic properties of structure II hydrates.

2. Method

2.1 Simulation tool and system definition

Molecular simulations were carried out using the Gromacs package version 4.5.4[61]. For the sII hydrates system, the cubic simulation box (34.62×34.62×34.62 Å initial dimensions, lattice parameter of a unit cell is 17.31 Å[50]) consisted of 2×2×2 unit cells. Periodic boundary conditions were used. The positions of the water oxygen atoms of the initial hydrate configuration were taken from x-ray crystallography, and the water hydrogen atoms were inserted to adjust the orientation for yield to Bernal-Fowler rule and minimize the net unit cell dipole moment and potential energy[62]. All guest molecules were placed at the center of the water cages, assuming that the propane and THF molecules both full occupied the large cages, and that the methane, carbon dioxide molecules fully lived in the small cages. The OPLS-AA all-atom[63] force field was used for both methane and propane. And the rigid, non-polarizable TraPPE potential[64-65] was used for CO_2 and THF molecules. Water was described by TIP4P/2005 model[66] , as this was found to

be suitable for the host-host interaction[40]. The particle-mesh Ewald (PME) summation method[67] was used to calculate the electrostatic interactions. Van der Waals interactions were calculated using the Lennard-Jones potential with a cut-off distance of 16 Å. The leapfrog algorithm[68] was employed to integrate the equation of motion with a 1 fs time step.

2.2 Simulation procedure

Isotropic *NPT* ensemble simulations were carried out to determine the average lattice parameters for pure propane and propane along with methane or carbon dioxide mixtures. Temperature and pressure control were implemented using velocity rescaling with a stochastic term[69] and Parrinello-Rahman extended-ensemble pressure coupling[70], respectively. For C_3H_8 pure and binary hydrates with CH_4 or CO_2 molecules, simulations were performed using the initial structure constructed above since the guest-host interaction is relatively weak. Contrarily, for the THF pure and binary hydrates with CH_4 or CO_2 molecules, longer simulation times were needed in the low temperature region because of the strong interaction between host and guest, as well as low kinetic energy. To increase the particle thermal motion and eliminate non-equilibrium states of system, a single annealing simulation was performed with 200ps to bring the clathrate hydrates to the desired volume and temperature before the MD simulation. All the simulation parameters were set as above. To simulate the temperature-dependent lattice parameter, the pressure was set to atmospheric pressure or 14.5 MPa, while the temperature varied from 5 to 270 K. To simulate the pressure-dependence of the lattice parameter, the temperature was set to the same value (287.15 K), and the pressure was varied from 10 to 100 MPa in steps of 10 MPa. This range of pressures covers most of the relevant conditions for the natural gas industry[71]. Afterwards, 10 ns production run simulations were performed in the *NPT* ensemble with 1 ns equilibration time.

It is known that classical MD simulations of lattice parameters of hydrates structures cannot capture accurately reported experimental results[40], particularly at temperatures below 150 K. Therefore, in order to decrease the deviation from experiments, a simple correction method developed by Costandy et al.[43-44], was used to modify lattice constants of the fully occupied structure sI with CH_4 or CO_2 pure hydrates. The corrected lattice constants were calculated from classical molecular dynamics simulations at low temperatures using the TIP4PQ/2005 water force field [72].The procedures are as follow: Step one, quantum path-integral simulation and classical simulation for empty sII structure have been performed using TIP4PQ/2005 water model[72] at temperature of 77, 100 and 125K. [73] Then the temperature dependence for density difference $C(T)$ ($= \rho_{empty}^{(CS)} - \rho_{empty}^{(PI)}$) was obtained by fitting the density deviation data of the two different simulations for the empty sII hydrates in the temperature range 77-125 K to a second degree polynomial: $C(T)=a_0+a_1T+a_2T^2$ with a_0=0.04672,a_1=-1.68913 $\times$ 10^{-4},a_2=2.17391 $\times$ 10^{-7}. Step two, classical MD simulations for C_3H_8 or THF pure and binary sII hydrates were performed using TIP4PQ/2005 water model as well as the other guest molecular force fields described above. Once the lattice constant a for a hydrates unit cell was available from classical MD simulations (CS), the hydrate density, ρ , was calculated through

$$\rho = \frac{n_w M_w + \sum_i^2 \theta_i v_i M_g}{N_{Av} V} \quad (1)$$

where n_w is the number of water molecules per hydrate unit cell, M is the molecular weight of water (w) and guest gas (g), N_{Av} is the Avogadro's number, θ_i is the fractional occupancy of cavity i by the gas

guest (θ_i = 0 or 1, propane or THF fully occupied in the large cages, CH_4 or CO_2 or empty for the small cages in structure sII), ν_i is the number of type *i* cavities in the unit cell, and $V = a^3$ is the hydrates unit cell volume. Step three, the hydrate density is corrected through the following equation: $\rho^{(corr)} = \rho - C(T)$, where *C(T)* was obtained in step one and superscript" corr" as a function of temperature. And then, we can substitute in Eqn. (1) the obtained value for ρ and re-solve it in order to calculate the corrected value for unit cell volume (V) and the lattice constant: $a^{corr}=(V^{corr})^{1/3}$. Finally, the lattice parameters performed by a series of similar *NPT* simulations and corrected by Costandy's approach were used to calculate the corresponding thermal expansion coefficients. Otherwise, the values of compressibility corresponding to different hydrates were determined by lattice parameters without Costandy's correction at constant temperature. All simulations were performed for propane hydrate, THF hydrates and these along with binary CO_2 or CH_4 within 5-287.15K and pressure range of 10-100MPa. The properties were obtained by numerical differentiation according to the following definitions:

$$\alpha_P = \frac{1}{V}\left(\frac{\partial V}{\partial T}\right)_P \quad (2)$$

$$\kappa_T = -\frac{1}{V}\left(\frac{\partial V}{\partial P}\right)_T \quad (3)$$

Where α_P is the thermal expansion coefficient, K^{-1}; k_T is the isothermal compressibility coefficient, MPa^{-1}; T is the temperature, K; P is the pressure, MPa^{-1} and V is the volume, $Å^3$.

Furthermore, we also used the fluctuations in the *NPT* ensemble to calculate the thermal expansion coefficients, isothermal compressibility and heat capacity of the single-crystal sII hydrate and compared these values with the numerical differentiation method and experimental values. The equations from fluctuation theory are as follows[74]:

$$\alpha_P = \frac{\left[\langle V \cdot U\rangle - \langle V\rangle \cdot \langle U\rangle + P\left(\langle V^2\rangle - \langle V\rangle^2\right)\right]}{k_B T^2 \langle V\rangle} \quad (4)$$

$$\kappa_T = \frac{1}{k_B T \langle V\rangle}\left(\langle V^2\rangle - \langle V\rangle^2\right)_{NPT} \quad (5)$$

$$C_P = \frac{ik_B N}{2} + \frac{1}{k_B T^2}\left[\begin{pmatrix}\langle U^2\rangle - \langle U\rangle^2 + \\ 2P\left(\langle V \cdot U\rangle - \langle V\rangle \cdot \langle U\rangle\right) \\ +P^2\left(\langle V^2\rangle - \langle V\rangle^2\right)\end{pmatrix}\right]_{NPT} \quad (6)$$

where k_B is Boltzmann's constant and equal to 1.38×10^{-23} J/K; U is the potential energy, J; C_P is the heat capacity at constant pressure, J/K; i is the number of degrees of freedom (i=3n-k, n is sample quantity and k is the number of constrained variables); and N is the number of molecules. The first term of Eqn (6) represents the contribution from the kinetic energy, and for a C_3H_8 or CH_4 molecule, i = 33 or 15, respectively; for a rigid CO_2 molecule, i = 5; for a THF molecule, TraPPE uses fixed bond lengths, i=10. Therefore, the first term of Equation (6) can be expressed as follows:

$$\frac{i}{2}k_BN=\frac{i}{2}k_BN_{H_2O}+\frac{15}{2}k_BN_{CH_4}+\frac{5}{2}k_BN_{CO_2}+\frac{33}{2}k_BN_{C_3H_8}$$
$$\frac{i}{2}k_BN=\frac{i}{2}k_BN_{H_2O}+\frac{15}{2}k_BN_{CH_4}+\frac{5}{2}k_BN_{CO_2}+\frac{10}{2}k_BN_{THF} \quad (7)$$

where i represents the number of degrees of freedom (DOF) of water molecules, N_{H_2O}, N_{CH_4}, N_{CO_2}, $N_{C_3H_8}$ and N_{THF} is the number of water molecules, methane molecules, carbon dioxide molecules, propane molecules and THF molecules, respectively. If the water molecules are fully mobile, then $i = 6$. If the water molecules can only rotate or only translate, then $i = 3$. If the water molecules are fully immobile, then $i = 0$. Here, we used i=6 because the water molecules can rotate and translate slightly in the hydrates structures. Usually, the heat capacity of gas hydrates is reported not in [J/K] but in [J/(kg·K)] or [J/(mol·K)], i.e., the specific heat capacity. Here, we denote the unit of specific heat capacity by [J/(kg·K)]:

$$c_p=\frac{1000N_AC_P}{Mn} \quad (8)$$

where c_p is the specific heat capacity, and N_A is Avogadro's constant. For an MD cell that consists of 2x2x2 unit cells, 1 mol MD cell contains 64 mol $C_3H_8 \cdot 17H_2O$ or $THF \cdot 17H_2O$ when the gases only fully occupy the large water cages and 64 mol $C_3H_8 \cdot 2CH_4$or$/CO_2 \cdot 17H_2O$ or $THF \cdot 2CH_4$or$/CO_2 \cdot 17H_2O$ when the gases fully occupy the water cages. Thus n=64. M is the molar mass (g/mol) of the gas hydrate.

3. Results and discussions

3.1 Lattice parameter and isobaric thermal expansion coefficient

In this section, we report first results of a series of simulations using TIP4P/2005 water model or TIP4PQ/2005 water model as well as guest molecular potentials mentioned above to determine the lattice parameters of structure II hydrates (C_3H_8 or THF pure sII hydrates and C_3H_8 or THF with CO_2 or CH_4 binary sII hydrates) as a function of temperature at atmospheric pressure or 14.5 MPa pressure. And then, we plot in Fig.1, the lattice parameters determined by TIP4PQ/2005 water model modified by Costandy's correction. The lattice parameters determined by TIP4P/2005 water model as well as experimental values of sII clathrate hydrates are also shown in fig.1. It is first observed that the calculated lattice parameters using the TIP4P/2005 water model vary in an almost linear manner with temperature at higher temperature (>200K). The linear variation stops below this temperature. Also, deviations between experimental[20, 75-76] and computational values become considerable in the low temperature region (<200K). The last leads us to conclude that quantum effects can have a significant effect on lattice parameter: The classical MD simulation using TIP4P/2005 water model could hardly reproduce the configurations at low temperatures[40, 43]. In contrast, the lattice parameters calculated by TIP4PQ/2005 water model and modified by Costandy's correction showed good agreement with the experimental data, also in the low temperature region. The TIP4P/2005 water model should therefore not be used to explain lattice constants in this temperature region. Unfortunately, this is the he region where natural gas hydrates are stable in sediments and pipelines [40]. Costandy's methodology is found to perform well, however, for cases of sII hydrates with single cage occupancies and for guest both without (for C_3H_8) and with (for THF) strong interaction between guest and host molecules.

Fig. 1 also shows that the lattice parameters of structure II C_3H_8 hydrates are smaller than structure II THF hydrate's and the lattice parameter increased when the small cages were occupied by secondary help-gas

species CH_4 and CO_2. Furthermore, compared with binary sII hydrates with CH_4 and pure hydrates, the binary sII hydrates with CO_2 expanding similar manners, especially in the high temperature region (>150K from Fig 1. In this study).

Ordinarily, guest molecules are enclathrated within the host water cages by weak van der Waals forces, and there is no strong interaction between the guest and host molecules. The push of the larger gas molecules on the cages is dominated by van der Waals repulsion, increasing by the size of the cages and therefore the size of the lattice. The maximum van der Waals diameters of propane and THF molecules were estimated using the Winmostar program[77]: 6.7Å for C_3H_8 and 6.5Å for THF. Despite the larger guest-size of C_3H_8 as compared to THF, Fig.1 shows that C_3H_8 hydrates has the smaller lattice parameters at the same temperature, which might be an evidence for the anomalous interaction between THF and host molecules in sII clathrate hydrates. In clathrate hydrates of guest with hydrophilic functional groups (THF), hydrogen bonds between the guest and the water molecules have been observed in MD simulation[55, 78] (Fig.2). The usual guest-host potentials encountered in parameterized versions of the van der Waals-Platteeuw equation do not take account of interactions such as guest-host hydrogen bonding, evidence for which was encountered recently both by experiment[57-58, 79] and theory[55, 80-81], Guest-host hydrogen bonding affects the guest to which the hydrogen bond is formed as well as the guests in neighboring cages which may have a Bjerrum defect in one of their cage faces. The host-guest interaction affects the structure of THF clathrate hydrate crystal and plays an important for the properties of clathrate hydrates. Figure1 also shows that the lattice parameters of hydrates with CO_2 in small cages were larger than those with CH_4 in the high temperature region (>150K in this study) under the same pressure condition. However, in the low temperature region (<150K in this study), the lattice parameters of C_3H_8 binary hydrates with CO_2 are much smaller than those with CH_4 under the same pressure condition. This is different from the result for THF binary hydrates. Those findings may imply that the lattice parameter is sensitive to the occupation of small cages and that the guest-guest interaction plays a role in the determination of the lattice parameter. Alavi's simulations[55] can be taken as support. They showed that the number and nature of the guest in the small cage affected the probability of hydrogen bonding of the tetrahydrofuran guest with the large cage water molecules. Hydrogen bonding of tetrahydrofuran in large cages occurs, despite the fact that the guests in the small cages do not themselves form hydrogen bonds with water. These results indicate that nearest neighbor guest-guest interactions (mediated through the water lattice framework) can affect the clathrate structure and stability. That is why the lattice parameter difference between THF binary hydrates with CO_2 and THF pure hydrates is larger than the same difference between C_3H_8 binary hydrates with CO_2 and C_3H_8 pure hydrates under the same temperature and pressure conditions. Overall, the host-guest interaction and guest-guest interaction both play important roles in the determination of the properties of clathrate hydrates, especially for THF pure and binary hydrate. A cautious remark in the end: It should be remembered that the simulations did only taken into account the intermolecular stretching, and not the intramolecular stretching, assuming it to be constant (both TIP4P/2005 and TIP4PQ/2005 water models are rigid water models). This may also partially explain the larger reported lattice constants in the high temperature region.

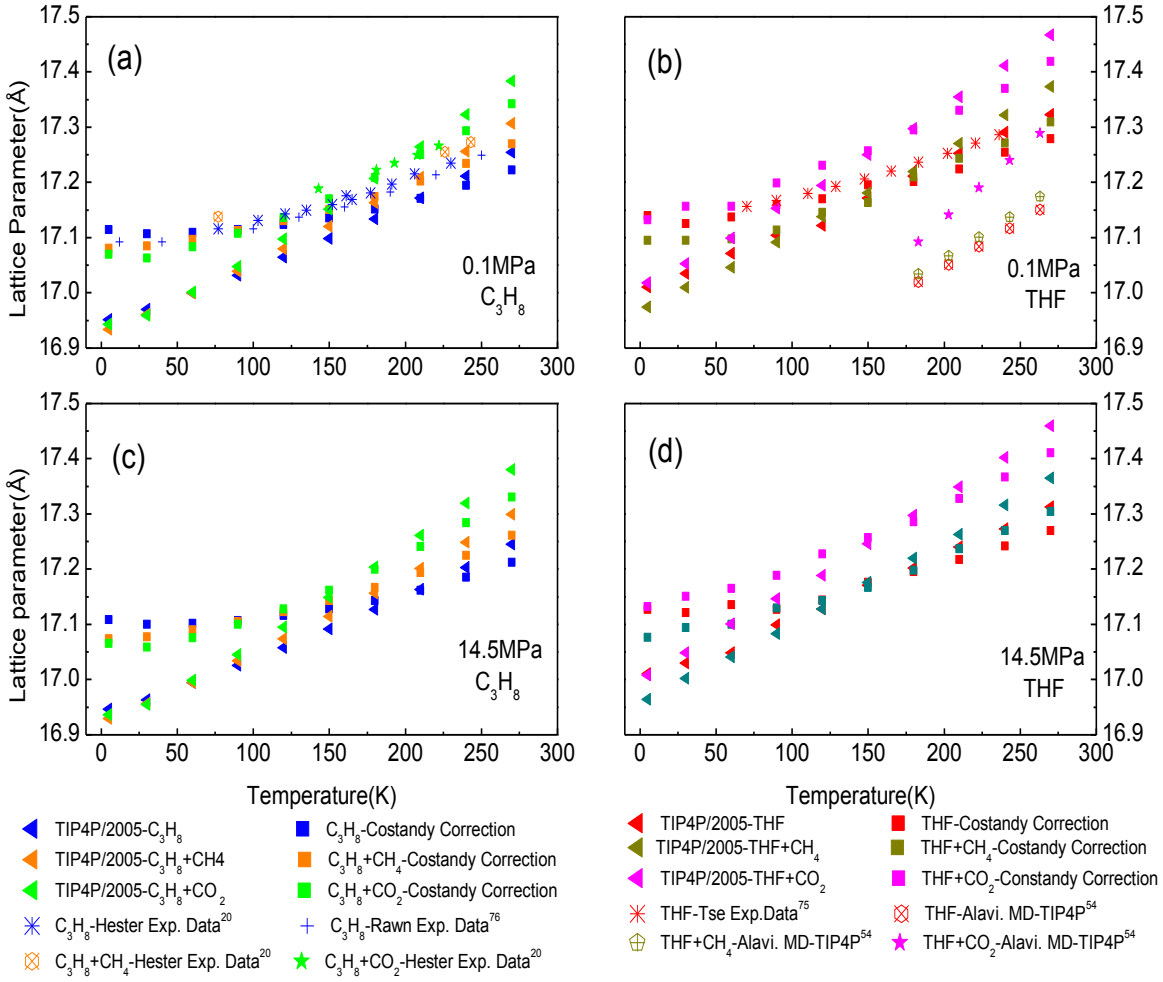

Fig.1 Lattice parameters for sII clathrate hydrates of the C_3H_8(a/c), THF(b/d) with different second-help molecules in the small cages as a function of temperature at atmospheric pressure (a/b) or 14.5 MPa (c/d) compared with the experimental values. Results are obtained by MD simulations, with (square points) and without (triangular points) the Costandy correction. Experimental data are shown as other signs. Data from other simulation works are indicated with a reference.

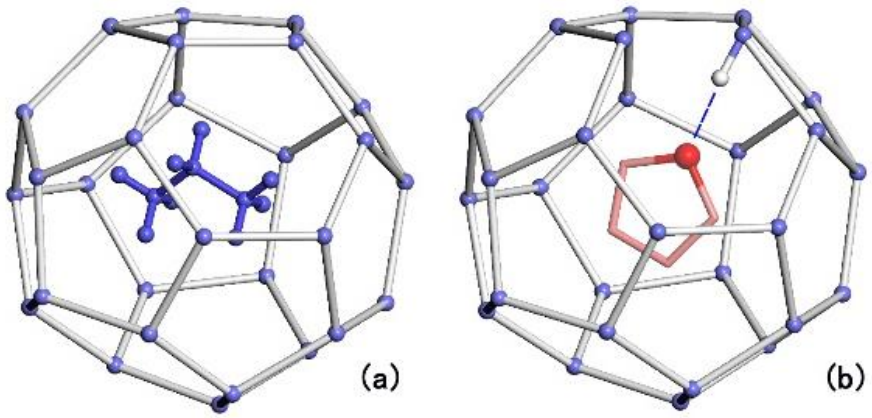

Fig2. Schematic representation of H_2O molecule cavities occupied by non-hydrogen bond forming guest C_3H_8(a) and hydrogen bond forming guest THF(b).

The volumes of the unit cells at atmospheric pressure or 14.5MPa were fitted to second-order polynomials as a function of temperature as follows:

$$V = B_2T^2 + B_1T + B_0 \quad (9)$$

Where V is the volume of the cell of the sII hydrate, in Å^3; and T is the temperature, in K; B_2, B_1, B_0 are coefficients of the second-order polynomial function. Their values for the different hydrates by two water models are presented in Tables I and II.

Table I Coefficients of polynomial function for the unit volume of sII hydrates at atmospheric pressure. (units B_2: Å^3/K^2; B_1: Å^3/K; B_0: Å^3)

	TIP4P/2005				TIP4PQ/2005 (and corrected)			
	B_2 ($\times10^{-4}$)	B_1	B_0	Determination Coeff.	B_2 ($\times10^{-4}$)	B_1	B_0	Determination Coeff.
C_3H_8	9.9244	0.7331	4865.9839	0.9998	0.0019	0.1551	5011.6093	0.9985
C_3H_8+CH_4	9.5216	0.9731	4850.7726	0.9999	0.0017	0.1615	4981.8777	0.9997
C_3H_8+CO_2	18.6	0.9979	4851.5848	0.9989	0.0025	0.2638	4964.4122	0.9971
THF	7.2386	0.8599	4917.7378	0.9965	0.0013	0.1343	5025.8891	0.9811
THF+CH_4	7.9961	1.1019	4886.4697	0.9994	0.0022	0.1365	4889.0561	0.9891
THF+CO_2	9.3672	1.2577	4921.6374	0.9997	0.0016	0.5090	5026.1473	0.9951

Table II Coefficients of polynomial function for unit volume of sII hydrates at 14.5 MPa pressure. (units B_2: Å^3/K^2; B_1: Å^3/K; B_0: Å^3)

	TIP4P/2005				TIP4PQ/2005 (and corrected)			
	B_2 ($\times10^{-4}$)	B_1	B_0	Determination Coeff.	B_2 ($\times10^{-4}$)	B_1	B_0	Determination Coeff.
C_3H_8	9.6815	0.7267	4861.4437	0.9997	0.0018	0.1642	5005.8863	0.9984
C_3H_8+CH_4	9.2894	0.9656	4846.9991	0.9999	0.0016	0.1661	4975.5149	0.9997
C_3H_8+CO_2	17.1	1.0437	4846.3404	0.9992	0.0025	0.2266	4960.7774	0.9965
THF	5.3119	0.8860	4912.2907	0.9962	0.0018	0.0013	5020.3309	0.9807

$THF+CH_4$	6.4517	1.1533	4877.3176	0.9997	0.0016	0.2971	4980.3069	0.9965
$THF+CO_2$	6.8359	1.3178	4915.3161	0.9995	0.0016	0.4942	5025.4776	0.9984

By combining those fits and eqn (2), the isobaric thermal expansion coefficient was determined as a function of temperature at atmosphere pressure or 14.5MPa pressure. Figure 3 shows the thermal expansion coefficient of the pure and binary hydrates, obtained from the numerical differentiation of eqn (9) for the two water models, compared with the value given by fluctuations in the *NPT* ensemble using TIP4P/2005 water model (Eqn (4)). The results from the fit to the polynomial and from the fluctuation method agree relatively well. Obviously, the value of the thermal expansion coefficient of the hydrates, calculated with the TIP4PQ/2005 water model and Costandy's correction, shows agreement with experimental data, especially in the low temperature region (<200K). The agreement generally increases when the small cages of sII structure hydrates are occupied by guest molecules at the same temperature. Both in C_3H_8 and THF binary hydrates, the thermal expansion coefficient of the binary hydrates with CO_2 guest molecular in small cages, is larger than when we include CH_4 binary hydrates at the same temperature. This finding agrees with the simulation results from the sI structure mixture hydrate[40] and is in contrast to an experimental report[20] (where the sample may be hampered by impurity). Many other measurements and MD simulations indicate that the thermal expansion coefficient of the CO_2 hydrate is larger than that of the Xe hydrates and that of the pure CH_4 hydrates at high temperature[28, 30, 40]. The symmetry and the configuration of extra-nuclear electrons, (CO_2 molecule has two Π-delocalized bonds) differ between CO_2 and CH_4 molecule. The difference causes stronger interactions between the host and the CO_2 molecules at high temperatures[27], and supports the idea that the host-guest interaction can play an important role in the determination of the properties of gas hydrates. However, both sI and sII structure hydrates are ice-like crystals in which the guest molecules are encapsulated in a network formed by hydrogen-bonded water molecules, and some similarities exist in the property of mechanics and thermodynamics, for example the host-host effect on expansion coefficient. That is the reason why the expansion coefficient of the pure propane hydrates is just slightly larger than the pure THF hydrate. In addition, when we compare Fig. 2(a) and Fig. 2(c) (or Fig. 2(b) and Fig. 2(d)), we find that the thermal expansion coefficient is not only temperature dependent, but also to some degree pressure dependent. The pressure does not have a substantial effect on the thermal expansion coefficient, however, so the effect of the intermolecular interactions on the temperature-dependent expansion coefficient may be more complex, than that on the pressure-dependent compressibility.

In conclusion, the guest – host interactions and guest-guest interactions may both play a similarly important role as the host – host interactions for hydrate expansion properties, similar to what is experimentally observed for thermal expansion behavior of sII clathrate hydrates with diatomic guest molecules[32]. This finding is in contrast to what was expected and may also explain the reason behind the difference in thermal expansion between sI and sII hydrates[20].

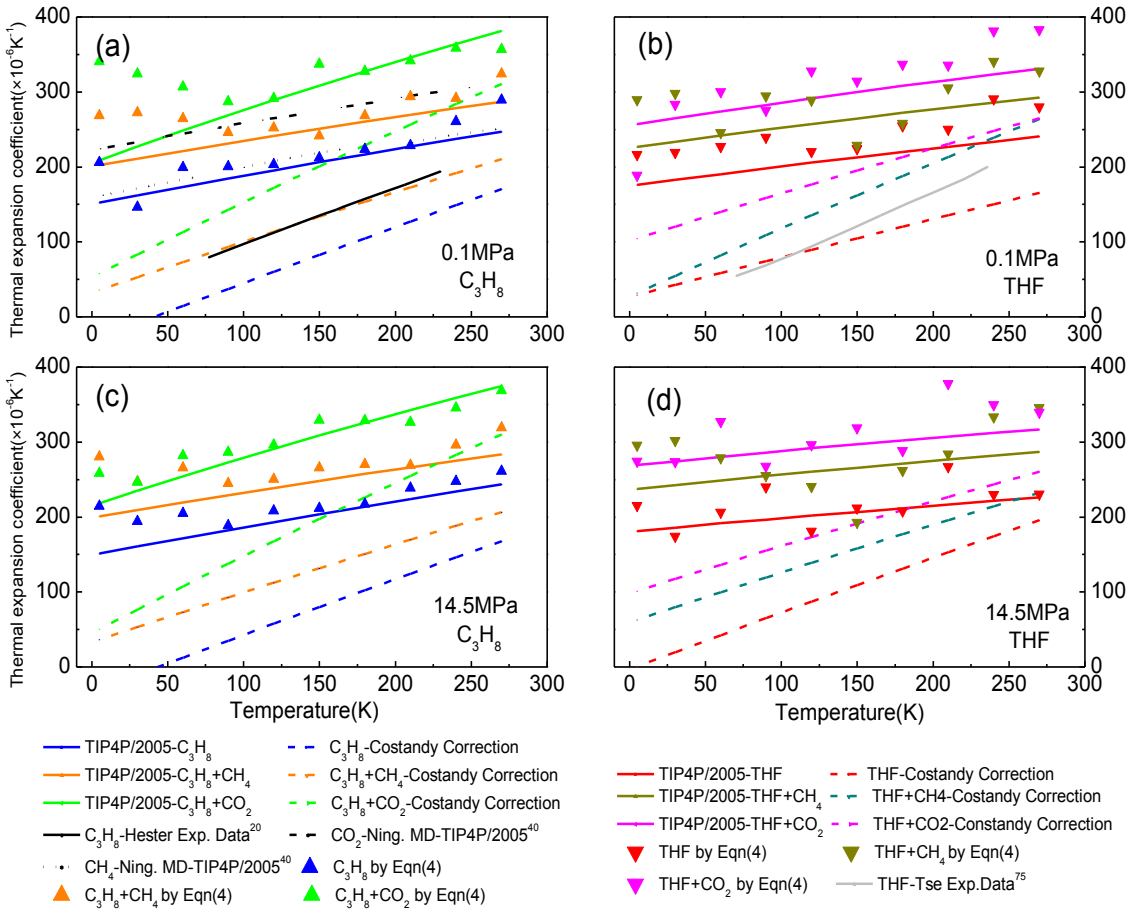

Fig 3. The isobaric thermal expansion coefficient for sII clathrate hydrates of the C_3H_8(a/c) or THF(b/d) with different guest molecular in the small cages as a function of temperature at atmospheric pressure(a/b) and 14.5MPa(c/d).

3.2 Isothermal compressibility

We used the TIP4P/2005 water model as well as guest molecular potentials described above to model the interactions at 287.15K. A series of simulations were performed to determine the isothermal compressibility as a function of hydrate compositions at various pressures (10 -100MPa) at the same temperature. The lattice parameters obtained are plotted in Fig. 4. The figure shows that the lattice parameter decreases with increasing pressure. At the maximum pressure of the simulation (100MPa), for the propane and THF pure hydrates, the deviations of unit cell volume was 1.0％and 1.3％ of the unit cell volume at 10MPa, respectively. The guest-host interaction and guest-guest interaction cannot vary much in this range. But, the parameters of binary THF hydrates are larger than those of binary C_3H_8 hydrates, in the presence of the same second-help molecules in small cages. Lattice parameters of propane and THF binary hydrates with CO_2 are furthermore larger than with CH_4 at the same pressure. This finding is in accordance with the results obtained above, and indicates that the lattice parameter of hydrates depends not only temperature and composition, but also on pressure.

The lattice parameters presented in Fig. 4 were fitted to second-order polynomials as follows:

$$
\begin{aligned}
V_{C_3H_8} &= 1.8935\times10^{-4}P^2 - 0.58P + 5159.9018 \\
V_{C_3H_8+CH_4} &= 2.1732\times10^{-4}P^2 - 0.5305P + 5211.8002 \\
V_{C_3H_8+CO_2} &= 2.1092\times10^{-4}P^2 - 0.6130P + 5286.8328 \\
V_{THF} &= 6.9879\times10^{-4}P^2 - 0.869P + 5219.6656 \\
V_{THF+CH_4} &= 5.2064\times10^{-4}P^2 - 0.6673P + 5270.0361 \\
V_{THF+CH_4} &= 3.8109\times10^{-4}P^2 - 0.70134P + 5366.2880 \\
10 \le P &\le 100 MPa
\end{aligned}
\qquad (10)
$$

Here V is the volume of the unit cell of the sII hydrate, in Å^3; and P is the pressure, in MPa. Using these expressions and eqn (3), we determined the isothermal compressibility. Figure 5 provides the values of the compressibility of the sII hydrates derived from the numerical differentiation of eqn (10) and from fluctuations in the *NPT* ensemble (eqn (5)). The results from the fit to the polynomial and from the fluctuation method again agree relatively well. We note that the C_3H_8 binary hydrates with CO_2 molecules in the small cages can be easier compressed than a C_3H_8 pure hydrate with small cages unoccupied. By contrast, it is more difficult to compress the C_3H_8 hydrates with CH_4 molecules filled in the small cages. We note that a gas hydrate occupied by a linear guest molecule appears to be more compressible than one occupied by a symmetric guest molecule. However, the isothermal compressibility of THF pure hydrates is relatively small due to the hydrogen-bonded framework. Defects inevitably found in real polycrystalline hydrate systems will increase compressibility. Meanwhile, the value of isothermal compressibility of the THF hydrates reduce approximately to the sI and sII structure number for small cages of hydrates crystal occupied by second-help guest molecules, such as CH_4 and CO_2. This finding shows that the so-called second-help guests could improve the stability of THF binary hydrates, even if the defect remain. Moreover, the THF binary hydrates with symmetric guest molecule (CH_4) is more difficult to compress than THF binary hydrates with linear guest molecule (CO_2), which however, is the same as propane binary hydrate.

The radial distribution functions (RDFs) were computed to further elucidate this point. The RDFs *goo* of host water are shown in Fig.6 for 14.5 MPa and 287.15 K for THF pure and binary hydrate with CH_4 or CO_2 as well as C_3H_8 pure. Those RDFs indicate that the arrangement of water molecules in C_3H_8 hydrates is more perfect than in THF hydrates. This may be attributed to the formation of crystallographic defects in THF hydrates, which could interrupt the regular pattern of symmetry or the equilibrium state of the crystal. Imperfection of the THF hydrate crystal may be a reason why it is abnormally easier to distort and compress than C_3H_8 hydrate. Interestingly, compared with C_3H_8 hydrates, THF with CH_4 binary hydrates are also present with a normal arrangement of water molecules, which is obviously different to the case of THF with CO_2 hydrates. Alavi's simulation[55] showed that the THF binary sII hydrates with CO_2 had the largest probability of hydrogen bond formation between guest THF and host water molecule. The pure THF sII hydrates with empty small cages had furthermore a greater probability of hydrogen bonding than the binary sII hydrates with CH_4. These findings may account for the distinct different arrangements of those hydrates. It was confirmed that the subtle guest-guest interaction could play an important role for the crystallographic structure and therefore affect the thermodynamic properties of hydrate crystals. Besides, THF and CO_2 binary hydrates have the largest probability to form hydrogen bonds, but they can also be stabilized by van der Waals forces between guest-host molecules and by subtle guest-guest interactions, even if THF and CO_2 binary hydrates are easier to compress than THF and CH4 binary hydrates (which are also stabilized by second-help molecules).

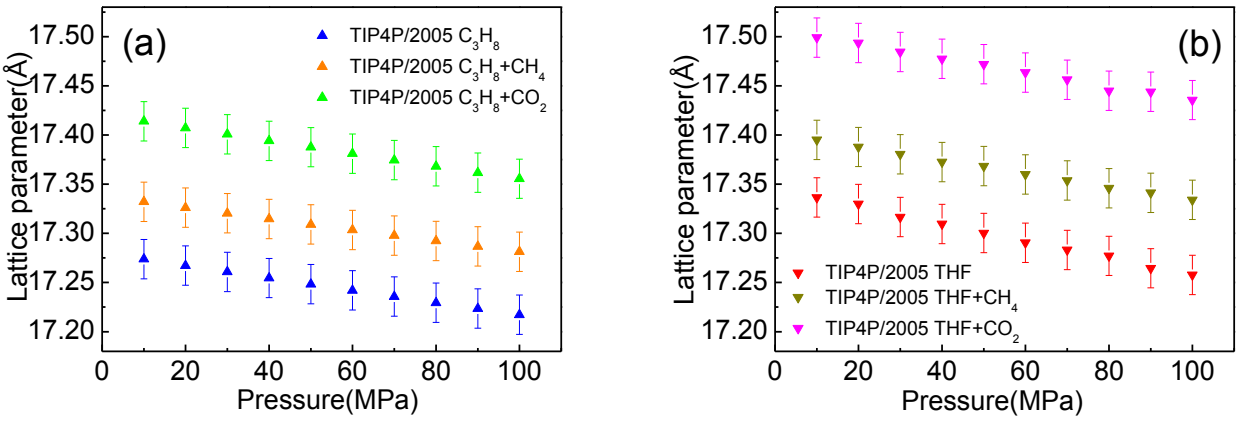

Fig.4 Lattice parameters for sII clathrate hydrates of C_3H_8(a) and THF(b) with different guest molecules in the small cages, as a function of pressure at 287.15K.

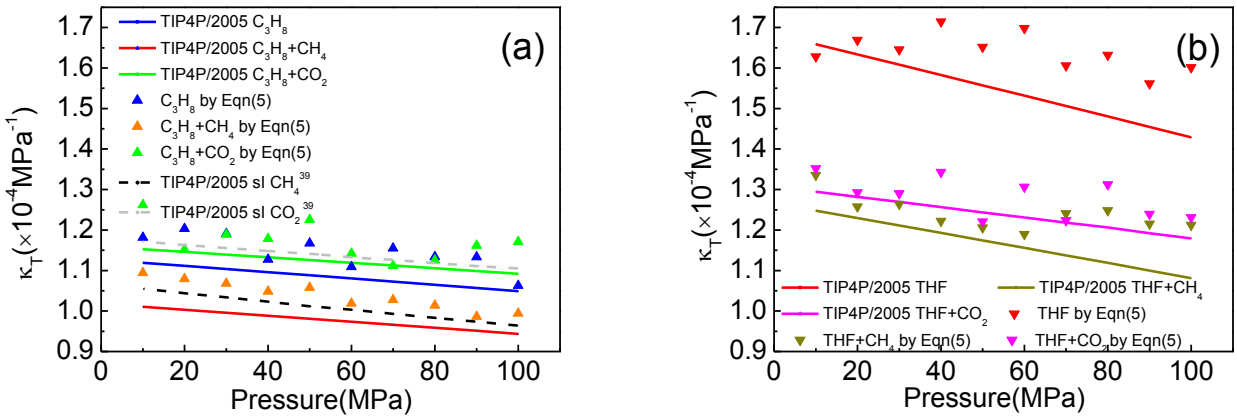

Fig.5 The isothermal compressibility of sII hydrates of C_3H_8(a) and THF(b) with different guest molecules in the small cages as a function of pressure at 287.15 K

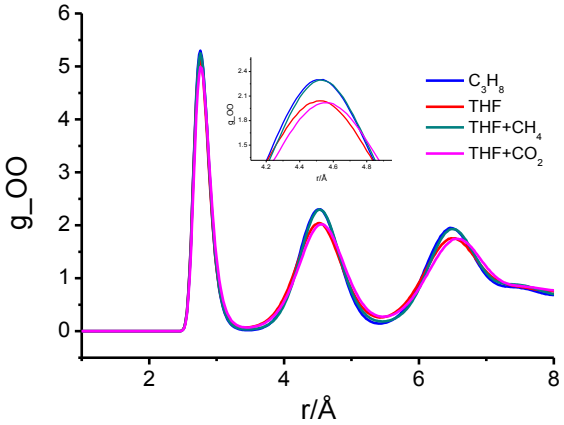

Fig.6 Radial distribution function (RDF) for the oxygen-oxygen atoms of water at 287.15K and 14.5MPa for different pure and mixed hydrates

The bulk modulus of clathrate hydrates is the inverse of the compressibility:

$$\beta_T = \frac{1}{\kappa_T} \qquad (11)$$

The bulk modulus of the propane sII structure hydrates and propane binary hydrates with CH_4, CO_2 from this relation is approximately 8.96 GPa, 9.93 GPa and 8.70 GPa at 287.15 K and 14.5 MPa, respectively. The calculated bulk moduli of propane hydrate, pure and binary, are close to the experimental value of ice Ih and sI CH_4 hydrate; approximately 9.1 GPa at 253 – 268 K and 9.1 GPa at 271K and 0.6 MPa,[33, 82] respectively. The bulk modulus of the propane sII structure hydrate decreased when CO_2 occupied the small cages. The effect should be considered for CH_4 recovery processes from CH_4 hydrates in deep oceans. This applies for instance to the Shenhu area, where sII structures are found in abundance. The knowledge is also relevant for the replacement of CH_4 by CO_2 in both sI and sII structure hydrates, especially when the solid including CH_4 hydrates act as cement or have a framework support function in porous sediments. Figure 5 shows the bulk modulus of the THF sII structure from Eq. 11 is approximately 6.0 GPa at 287.15K and 14.5 MPa, which is far apart from values of other sI and sII hydrates. It reflects that pure THF hydrates under this condition are relatively soft, probably due to a defective hydrogen-bonded framework. When the small cages of THF hydrates were filled with second-help molecules CH_4 or CO_2, the bulk modulus increased to 8.1 GPa and 7.8 GPa at 287.15 K and 14.5 MPa, respectively.

The results taken together indicate that small cage - guests can stabilize the structure through hydrogen binding of THF in binary structure II clathrate hydrates. Since the bulk modulus is mainly determined by the elasticity of the hydrogen-bonded water framework, the effect of small cage guests should not be neglected. Variable filling of the cavities with guest molecules also has a substantial effect on the bulk modulus, especially for hydrates with strong guest-host interaction.

3.3 Specific heat capacity at constant pressure

The specific heat capacity at constant pressure is used to compute hydrate entropy and enthalpy as a function of temperature. With information also on the enthalpies of phase transition, one can predict hydrate stability. In the permafrost region, the temperature of the hydrate deposits is normally far from the equilibrium temperature. Knowledge of the limit for stability is essential for prediction of climate gas depletion.[83] So far, specific heat capacity has been measured for propane[37] and tetrahydrofuran[39, 84-85] hydrates. There are limited data for sII structure binary hydrates with CH_4 and CO_2 molecules. The results and discussion above have shown that the fluctuation method can give results comparable to those calculated by the fitting method. Therefore, the fluctuation method was used to also calculate the average heat capacities of the C_3H_8 and THF sII structure pure hydrates and their binary mixtures. We calculated the constant pressure specific heat capacity of the mixed hydrates in the temperature range 5 - 287.15 K and the pressure range 10-100 MPa. The results were plotted in Fig. 7 and 8 and compared to published result for sII hydrates. We see that the different clathrate hydrates have relatively different heat capacities. The specific heat capacities of the C_3H_8 hydrates are slight larger than those of the THF hydrates. We explain that by the guest molecule property and the interaction between guest and host. Compared with the pure C_3H_8 and THF hydrates, the specific heat capacity of both C_3H_8 and THF hydrates decrease when the small cages of hydrates are occupied by CO_2 molecules and they increase when the same cages are filled with CH_4 molecules at the same temperature and pressure. That is, the effect of the CO_2 molecule can be treated as a positive contribution to the heat capacity in sII structure hydrates, while the CH_4 molecule has a negative

contribution relatively speaking. This is in accordance with the result published on sI hydrates[40]. With increasing pressure, the heat capacities decrease slightly. The heat capacity of C_3H_8 or THF pure and binary hydrates as a function of pressure at 287.15K was fitted to a line as follows:

$$c_{P\,C_3H_8} = -0.7563P + 3613.2690 \qquad c_{P\,\mathrm{THF}} = 2.7669P + 3585.7779$$
$$c_{P\,C_3H_8+CH_4} = -0.4813P + 3717.0008 \qquad c_{P\,\mathrm{THF}+CH_4} = -0.3824P + 3215.7374 \qquad (12)$$
$$c_{P\,C_3H_8+CO_2} = -0.1763P + 3189.2362 \qquad c_{P\,\mathrm{THF}+CO_2} = -0.0559P + 2764.3700$$
$$(10 \le \mathrm{P} \le 100\mathrm{MPa})$$

Here c_p is the specific heat capacity at constant temperature, in J kg^{-1} K^{-1}, and P is pressure, in MPa. According to the eqn (12), the specific heats of C_3H_8, C_3H_8 with CH_4 and C_3H_8 with CO_2 hydrates are in the range of 3605-3537.6 J kg^{-1} K^{-1}, 3712-3668.8 J kg^{-1} K^{-1} and 3187-3171.6 J kg^{-1} K^{-1}, respectively, and decrease by approximately 1.9%, 1.1% and 0.5% between 10 and 100 MPa, respectively.

The above analyses show that the specific heat capacity of sII structure is (relatively) pressure independent. The pressure has a complicated effect on the heat capacities of the THF sII structure hydrates. As the pressure increased, the value of heat capacity of THF pure hydrates apparently increase by 6.9%. But, when the small cages of THF hydrates are occupied by small molecules, such as CH_4 and CO_2, the heat capacity of the binary hydrates may decease slightly with the pressure increase. This finding may be attributed to the subtle guest-guest interaction and lattice defects, which can affect the thermal motion of atoms and then distort the specific heat capacity. Likewise, according to the eqn (12), the specific heats of THF with CH_4 and THF with CO_2 hydrates are in the range of 3211-3199.7 J Kg^{-1} K^{-1} and 2764-2766.7 J Kg^{-1} K^{-1}, respectively, and decrease by approximately 0.4% and 0.1% between 10 and 100MPa.

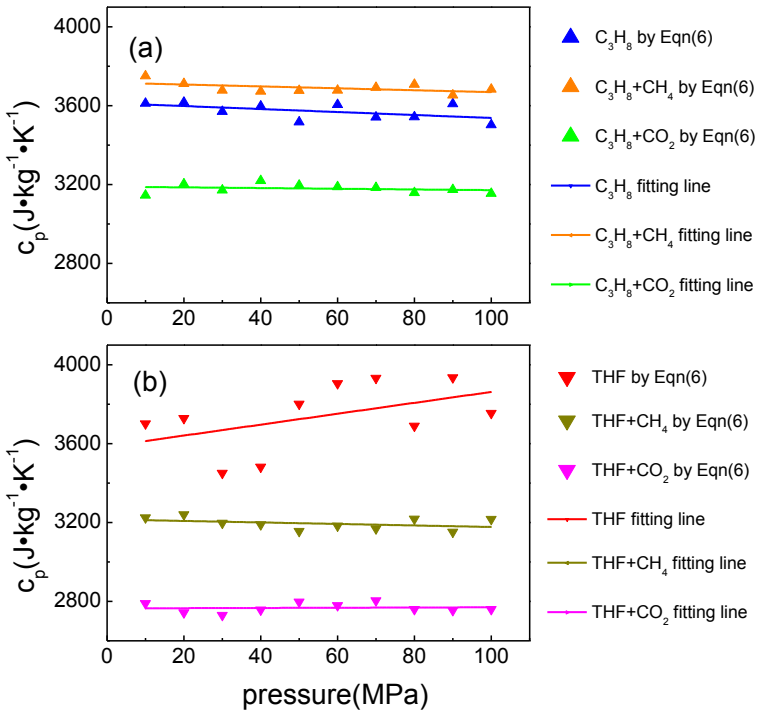

Fig.7 Pressure dependence of the specific heat capacity at constant pressure of C_3H_8(a), THF(b) pure and with CH_4 or CO_2 binary hydrates at 287.15K.

Compared with the pressure, the effect of temperature on the specific heat is larger. Handa[37, 86] obtained approximately 804-2027 J kg^{-1} K^{-1} for propane sII hydrates (C_3H_8 • $17H_2O$ refers to full occupancy of the large cages of structure II) between 85 and 279 K at 0.34 MPa and 841-2074 J kg^{-1} K^{-1} for THF pure hydrates (THF • $16.9H_2O$) between 85 and 270 K. The capacity increased 152.1% within this temperature range. Leaist et al.[39] investigated approximately 1066-1893 J kg^{-1} K^{-1} for THF hydrate (THF • $16.9H_2O$) between 120-260K at atmospheric pressure. The value increased 77.6% in the temperature interval of 10 K. Yamamuro et al.[84] measured approximately 56.7-4025.2 J kg^{-1} K^{-1} for THF pure hydrates (THF.$16.64H_2O$) between 12-300K at atmospheric pressure. Tombari et al.[85] measured and compared the heat capacity of the THF clathrate hydrates and of its components (THF • $15.9H_2O$, THF • $17.1H_2O$ and THF • $17.7H_2O$) against the temperature at ambient pressure. Our simulations indicated that the heat capacity of C_3H_8 or THF - pure and binary hydrates as a function of temperature at 14.5MPa can be approximately fitted to a line as follows:

$$\begin{aligned} c_{P\,C_3H_8} &= 1.5018T + 3071.3113 & c_{P\,\mathrm{THF}} &= 2.1112T + 2412.7323 \\ c_{P\,C_3H_8+CH_4} &= 0.9386T + 3368.7513 & c_{P\,\mathrm{THF}+CH_4} &= 1.4161T + 2760.1949 \\ c_{P\,C_3H_8+CO_2} &= 1.4115T + 2675.4371 & c_{P\,\mathrm{THF}+CO_2} &= 1.9013T + 2358.7803 \end{aligned} \qquad (13)$$

$$(5 \le T \le 270K)$$

Where c_p is the specific heat capacity at constant pressure, in J kg^{-1} K^{-1}, and T is the temperature in K. The average value of the heat capacity of C_3H_8 pure hydrates increase approximately 8% from 3261 J kg^{-1} K^{-1} at 150K to 3522 J kg^{-1} K^{-1} at 270K. The value of the heat capacity of THF pure hydrates increased approximately 15.2% in the same temperature region. The increase rate of the heat capacity of pure THF hydrates is the largest of those hydrates mentioned in this paper. The RDFs for oxygen-oxygen of water and oxygen atom of THF with the hydrogen atom of water (HW) at 14.5MPa pressure for the THF pure sII hydrates were shown in Fig.9. The insert shows the THF-water hydrogen bonding in the THF hydrates as the area under the peak in the RDF at 1.5Å. The peak is related to the extent of THF-water hydrogen bonding in THF hydrates. The guest-host hydrogen bonding gradually degrades with increasing of temperature and decreasing activation barrier to motion of THF molecules.[87-88] The water molecules of the framework become more labile and the heat capacity increases rapidly for THF hydrates after the melting temperature (287.15K).

Although the results yield similar dependencies on temperature, there is a systematic difference between the experimental values and the calculated of heat capacities of C_3H_8 and THF pure hydrates, especially at low temperature. We have calculated the value of the specific heat capacity of liquid water at 298 K and 1 atm using the TIP4P/2005 water model. The value was 84.6 J mol^{-1} K^{-1}, approximately 12% larger than the experimental value, 75.6 J mol^{-1} K^{-1}. [40] The specific heats of C_3H_8, THF pure and binary hydrates in this case may be similarly overestimated (see the ESI. Compared two different fluctuation methods). Considering the systematic deviation, the calculated values were in the range of 3219-3158.0 J kg^{-1} K^{-1} for C_3H_8 pure hydrates, 3314-3275.9 J kg^{-1} K^{-1} for C_3H_8 binary hydrates with CH_4 and 2846-2831.2 J kg^{-1} K^{-1} for C_3H_8 binary hydrates with CO_2 at 287.15K between 10 and 100 MPa and 2749-3104.3 J kg^{-1} K^{-1} 3011-3233.2 J kg^{-1} K^{-1} 2394-2729.1 J kg^{-1} K^{-1} at 14.5 MPa between 5 and 270 K, respectively. Considering the temperature or pressure difference between the measurements and our simulations, the modified results are still higher than the experimental measurements at a high temperature range. The experiments may have been hampered by the impurity of the hydrates samples. Although the effect of residual ice or liquid water on the measurements can be eliminated,[17, 89] the residual gas is barely removed because the samples,

whether synthesized in a laboratory or obtained in nature, contain many micro-pores.[90-92] The diameter of these pores was 100 – 500 nm, sometimes even 1 μm.[92] In addition, it is more difficult to compress polycrystalline hydrates samples with multiple pores than polycrystalline ice with multiple pores. Therefore, the micro-pores and residual gas may greatly lower the experimental values of the specific heat of gas hydrates. Furthermore, the cages in the gas hydrates in the lab and in nature may not be fully occupied by guest molecules (sometimes water-deficient and therefore excess guest molecules). And the cage occupancy also depends upon the temperature, pressure, guest concentration and the guest and cage types. However, the cage occupancy has a complicated and weak effect on the heat capacities of hydrates at different pressure.[40]

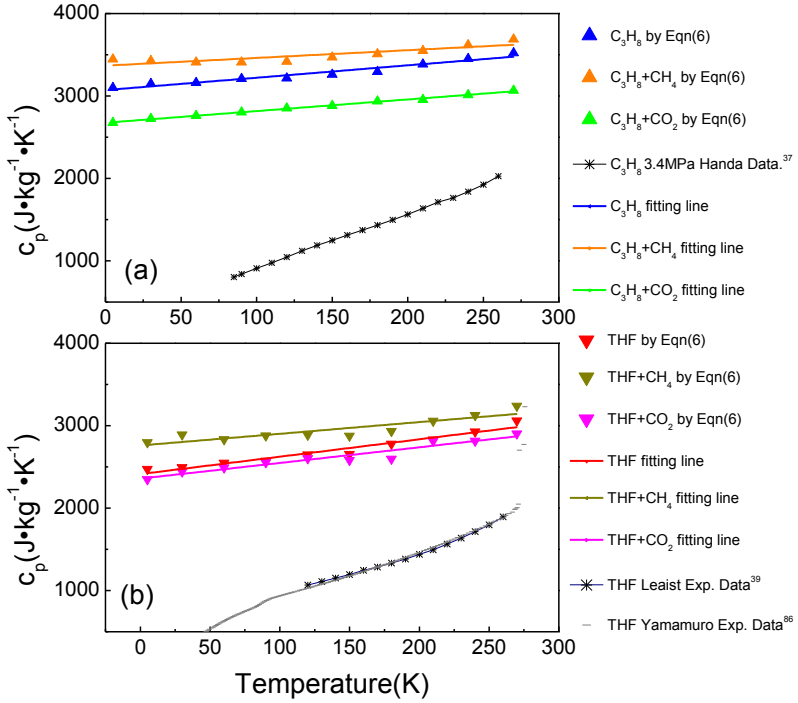

Fig.8 Temperature dependence of specific heat capacity of C_3H_8(a) or THF(b) pure and binary hydrates with CH_4 or CO_2 binary hydrates at 14.5MPa.

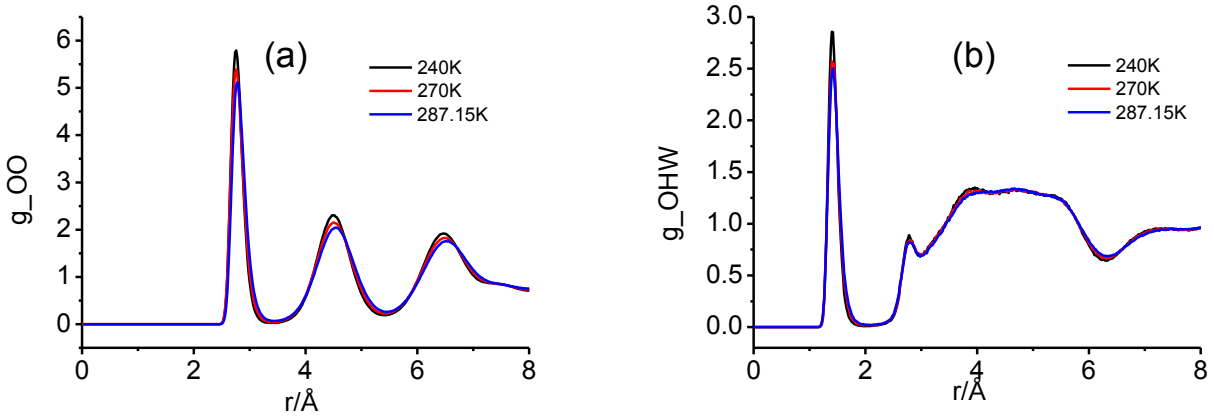

Fig.9 Radial distribution functions for the oxygen-oxygen atom of water(a) and the oxygen atom of THF(O)

with the hydrogen atom of water (HW) at 14.5MPa(b) pressure for the THF pure sII hydrates.

4. Discussion

According to our simulations, the host-host interaction, guest-host interaction and guest-guest interaction all have effects on the expansion, compressibility and heat capacity of gas hydrates. Generally, the host-host interaction plays the main role for mechanical and thermal properties of both structure I and II clathrate hydrates at lower temperatures (≤ 200K) and pressures (≤100 MPa). The relatively weaker guest-host interaction has an impact on the properties at higher temperatures and pressures. However, the guest-host and guest-guest interaction appears different for thermal and mechanical behavior of gas hydrates, especially for hydrates with hydrophilic guest molecules, in which the guests may form hydrogen bonds with the cage water (leading to the formation of a Bjerrum L-defects between two framework water molecules). The mechanical and thermal properties of hydrates with these extra hydrogen-bonded frameworks follow special patterns. While other sI and sII clathrate hydrates with hydrophobic molecules, obtain a stronger guest-host and guest-guest coupling interaction (≥260K) and obtain an extraordinarily high strength compared with other icy compounds.[93]

Two water models, TIP4P/2005 and TIP4PQ2005, were used in our simulations. Compared with the experimental results, the lattice parameters calculated using TIP4P/2005 water model exhibit a discrepancy with the experimental values below 200K, similar to what was observed for sI and sH hydrates. Subsequently, we modified the lattice parameters using Costandy's method, leading to a match with the experimental value at the low temperatures (Fig.1). As a result, the deviation between the calculated thermal expansion coefficient and the experimental values, which was large using TIP4P/2005 water model, could be reduced significantly. To some extent, the specific heat capacities calculated by our simulations deviate from experimental values below 260 K (Fig. 8). This behavior may imply that the rigid and non-polarizable water models and guest potentials do not describe properly the host–guest interaction. As mentioned above, the host-guest and guest-guest interactions are rather weak. Random thermal motions of the host and guest molecules are constrained under low-temperature conditions, but not at high. Hydrate proton NMR analysis and dielectric constant measurements have suggested that water molecular motion is "frozen in" at very low temperatures (<50 K) so that hydrates lattices become rigid.[94] The reorientation of water molecules is the first-order contribution to water motion in the structure; the second-order contribution is due to translational diffusion at these low temperatures. The rate of molecular water diffusion is as much as two orders of magnitude slower in the gas hydrates than in ice.

Supplementary calculations indicated that a smaller number of degrees of freedom i(DOF) of water molecules in hydrates may be more suitable for determination of the heat capacity by the fluctuation method at lower temperatures, especially in the solid state of the water-related system. For example, above 271.15 K, i = 3 can result in a c_P of water or C_3H_8 and THF pure hydrates that is closer to the experimental values. However, i = 0 may be more suitable for ice Ih or C_3H_8, THF pure hydrates at lower temperatures and can yield a c_P value that is closer to the experimental values (Fig. 10).

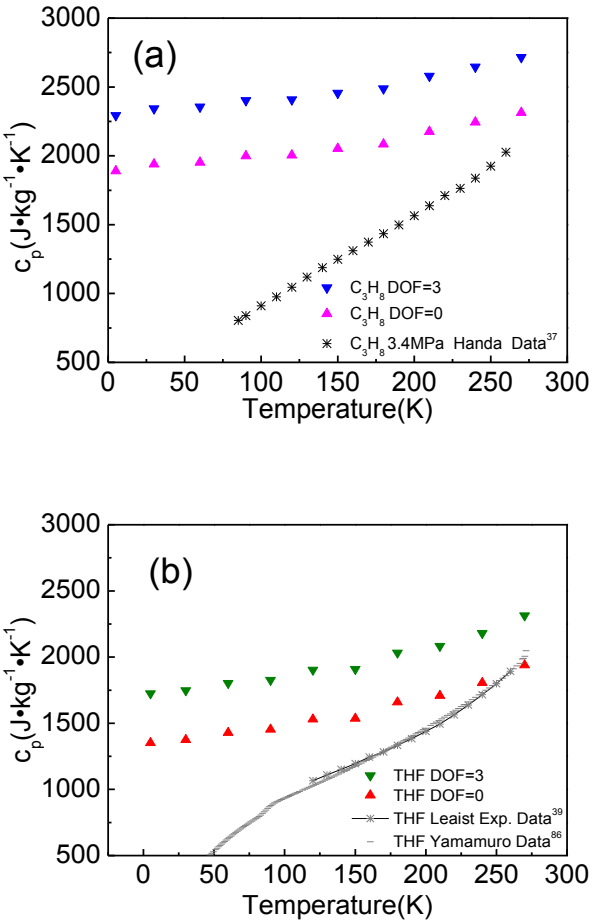

Fig.10 Temperature dependence of specific heat capacity of C_3H_8(a) and THF(b) pure hydrates at 14.5MPa using DOF=0 and 3.

Experiments[89, 93] have shown that polycrystalline sI hydrates are ductile and that sII hydrates exhibit an irreversible plastic-deformation-like pattern, where the expanded lattices fail to recover their original state with contraction. The tendency of thermal expansion appears to be "memorized" from previous history. Therefore, to gain a better understanding of these properties of gas hydrates, it is necessary to use more realistic intermolecular potentials and more complex approximations that consider the inharmonic effects, although such undertakings will require a substantial calculation time. A suitable description of the intermolecular interactions of the guest – guest and guest – host complexes is also important in the study of simulated properties of gas hydrates, considering the importance of the guest – host coupling interaction on the thermodynamic properties of C_3H_8 or THF hydrates. A highly accurate and explicit model for the guest – water interaction potential is required, and the use of LJ parameters fitted to the ab initio data does provide a good approach. But in our further studies, polarizable water models and ab initio-fit H_2O-C_3H_8 or THF potentials will be tested by studying the effects of temperature and occupancy on the thermal and mechanical properties of monocrystalline and polycrystalline gas hydrates, and the results will be compared to those from ab initio density functional theory.

5. Conclusions

Classical molecular simulations were performed to determine mechanical and thermodynamic properties

of structure II C_3H_8 or THF pure and binary hydrates, including thermal expansion coefficient, isothermal compressibility and heat capacity at constant pressure. For THF pure and binary hydrates, a short single annealing simulation was first done to optimize the initio configuration at low temperature, with the intention to make the initial structure more reasonable and decrease the simulation time.

We found that the correction for lattice parameters of hydrates in low temperature region is significant improvement of the results compared to experimental data. This simple methodology to incorporate quantum effects is found to perform well both in C_3H_8 and THF hydrates at low temperature and achieves a balance between relatively accurate results and low computational time. Based on above operation and the correction, the lattice parameters and thermal expansion coefficients of C_3H_8 and THF hydrates are close to the experimental values. The results provide a basis for further study of the effect of temperature and guest molecule types on the expansion at low temperature by MD simulations. Our simulations also reveal that the lattice parameter at a constant pressure or a constant temperature varies as a function of the guest type and guest coupling interaction. The thermodynamic properties of THF hydrates are similar to that of C_3H_8 hydrates and CH_4 hydrates except for compressibility, which also provides the possibility for the application of THF hydrates instead of other hydrates in the experiment. Small molecules, such as CH_4 and CO_2, play an obvious role in the stabilization of THF hydrates structure with defect. Moreover, when the CO_2 molecules replace CH_4 molecules in the small cages of sII structure, the lattice parameters, isothermal compressibility and thermal expansion of the hydrates increase, and the bulk modulus and specific heat capacity decrease accordingly. The effect to structure II hydrates is the same as that to structure I hydrates, that is, this effect has nothing to do with crystal structure and other guest type in the hydrates. Furthermore, the effect of the hydrates volume and heat capacity variations should not be neglected during the recovery of CH_4 from CH_4 hydrates in deep oceans using CO_2 to replace CH_4, especially in the calculation of phase equilibria and mechanical stability of sediments.

Although the heat capacities of C_3H_8, THF pure and binary hydrates using the fluctuation method showed a systematic deviation from the experimental values at lower temperatures, the results are still comparable with the experimental values at higher temperatures, and in reality, most natural hydrates reservoirs and petroleum industry temperatures are in the higher temperature range. The present approach, which can replace the costly and time-consuming experimental measurements and be applied to calculate the variation of mechanical and thermal properties mixture hydrates with different guest types, could potentially be applied to other complex hydrates systems, such as sI + sII hydrates; gas storage and transportation; and deep-sea sequestration of CO_2.

Acknowledgements

This work was supported by National High-Level Talent Special Support Plan, the National Natural Science Foundation of China (41672367), Fok Ying Tong Education Foundation (132019), and China Geological Survey Project (DD20160216). High Performance Computing Center of CUG is acknowledged for the computing resource. The work was partly supported by the Research Council of Norway through its Centres of Excellence funding scheme, project number 262644 PoreLab and TJHV acknowledges NWO-CW for a VICI grant.

References

1. Jr, E. D. S.; Koh, C. A., Clathrate Hydrates of Natural Gases. *Crc Press* **2007**.

2. Ripmeester, J. A.; Tse, J. S.; Ratcliffe, C. I.; Powell, B. M., A New Clathrate Hydrate Structure. *Nature* **1987**, *325*, 135-136.
3. Tohidi, B.; Danesh, A.; Todd, A. C.; Burgass, R. W., Hydrate-Free Zone for Synthetic and Real Reservoir Fluids in the Presence of Saline Water. *Chem Eng Sci* **1997**, *52*, 3257-3263.
4. Florusse, L. J.; Peters, C. J.; Schoonman, J.; Hester, K. C.; Koh, C. A.; Dec, S. F.; Marsh, K. N.; Sloan, E. D., Stable Low-Pressure Hydrogen Clusters Stored in a Binary Clathrate Hydrate. *Science* **2004**, *306*, 469-471.
5. Kvenvolden, K. A., Gas Hydrates - Geological Perspective and Global Change. *Rev Geophys* **1993**, *31*, 173-187.
6. Yoon, J. H.; Kawamura, T.; Yamamoto, Y.; Komai, T., Transformation of Methane Hydrate to Carbon Dioxide Hydrate: In Situ Raman Spectroscopic Observations. *J Phys Chem A* **2004**, *108*, 5057-5059.
7. Koh, C. A., Towards a Fundamental Understanding of Natural Gas Hydrates. *Chem Soc Rev* **2002**, *31*, 157-167.
8. Sum, A. K.; Koh, C. A.; Sloan, E. D., Clathrate Hydrates: From Laboratory Science to Engineering Practice. *Ind Eng Chem Res* **2009**, *48*, 7457-7465.
9. Mao, W. L.; Mao, H. K.; Goncharov, A. F.; Struzhkin, V. V.; Guo, Q. Z.; Hu, J. Z.; Shu, J. F.; Hemley, R. J.; Somayazulu, M.; Zhao, Y. S., Hydrogen Clusters in Clathrate Hydrate. *Science* **2002**, *297*, 2247-2249.
10. Lee, H.; Lee, J. W.; Kim, D. Y.; Park, J.; Seo, Y. T.; Zeng, H.; Moudrakovski, I. L.; Ratcliffe, C. I.; Ripmeester, J. A., Tuning Clathrate Hydrates for Hydrogen Storage. *Nature* **2005**, *434*, 743-746.
11. Nakajima, T.; Akatsu, S.; Ohmura, R.; Takeya, S.; Mori, Y. H., Molecular Storage of Ozone in a Clathrate Hydrate Formed from an O-3+O-2+Co2 Gas Mixture. *Angew Chem Int Edit* **2011**, *50*, 10340-10343.
12. Grim, R. G.; Kerkar, P. B.; Shebowich, M.; Arias, M.; Sloan, E. D.; Koh, C. A.; Sum, A. K., Synthesis and Characterization of Si Clathrate Hydrates Containing Hydrogen. *J Phys Chem C* **2012**, *116*, 18557-18563.
13. Koh, D. Y.; Kang, H.; Jeon, J.; Ahn, Y. H.; Park, Y.; Kim, H.; Lee, H., Tuning Cage Dimension in Clathrate Hydrates for Hydrogen Multiple Occupancy. *J Phys Chem C* **2014**, *118*, 3324-3330.
14. Sloan, E. D., Introductory Overview: Hydrate Knowledge Development. *Am Mineral* **2004**, *89*, 1155-1161.
15. Ning, F. L.; Yu, Y. B.; Kjelstrup, S.; Vlugt, T. J. H.; Glavatskiy, K., Mechanical Properties of Clathrate Hydrates: Status and Perspectives. *Energ Environ Sci* **2012**, *5*, 6779-6795.
16. Yuan, T.; Spence, G. D.; Hyndman, R. D.; Minshull, T. A.; Singh, S. C., Seismic Velocity Studies of a Gas Hydrate Bottom-Simulating Reflector on the Northern Cascadia Continental Margin: Amplitude Modeling and Full Waveform Inversion. *J Geophys Res-Sol Ea* **1999**, *104*, 1179-1191.
17. Waite, W. F.; Stern, L. A.; Kirby, S. H.; Winters, W. J.; Mason, D. H., Simultaneous Determination of Thermal Conductivity, Thermal Diffusivity and Specific Heat in Si Methane Hydrate. *Geophys J Int* **2007**, *169*, 767-774.
18. Koh, C. A.; Sloan, E. D.; Sum, A. K.; Wu, D. T., Fundamentals and Applications of Gas Hydrates. *Annu Rev Chem Biomol* **2011**, *2*, 237-257.
19. Tse, J. S.; Shpakov, V. P.; Belosludov, V. R.; Trouw, F.; Handa, Y. P.; Press, W., Coupling of Localized Guest Vibrations with the Lattice Modes in Clathrate Hydrates. *Europhys Lett* **2001**, *54*, 354-360.
20. Hester, K. C.; Huo, Z.; Ballard, A. L.; Koh, C. A.; Miller, K. T.; Sloan, E. D., Thermal Expansivity for Si and Sii Clathrate Hydrates. *J Phys Chem B* **2007**, *111*, 8830-8835.
21. Tse, J. S.; White, M. A., Origin of Glassy Crystalline Behavior in the Thermal-Properties of Clathrate Hydrates - a Thermal-Conductivity Study of Tetrahydrofuran Hydrate. *J Phys Chem-Us* **1988**, *92*, 5006-5011.
22. Tse, J. S.; Klug, D. D.; Zhao, J. Y.; Sturhahn, W.; Alp, E. E.; Baumert, J.; Gutt, C.; Johnson, M. R.; Press, W., Anharmonic Motions of Kr in the Clathrate Hydrate. *Nat Mater* **2005**, *4*, 917-921.

23. Marchi, M.; Mountain, R. D., Thermal-Expansion of a Structure-Ii Hydrate Using Constant Pressure Molecular-Dynamics. *J Chem Phys* **1987**, *86*, 6454-6455.
24. Rosenbaum, E. J.; English, N. J.; Johnson, J. K.; Shaw, D. W.; Warzinski, R. P., Thermal Conductivity of Methane Hydrate from Experiment and Molecular Simulation. *J Phys Chem B* **2007**, *111*, 13194-13205.
25. Schober, H.; Itoh, H.; Klapproth, A.; Chihaia, V.; Kuhs, W. F., Guest-Host Coupling and Anharmonicity in Clathrate Hydrates. *Eur Phys J E* **2003**, *12*, 41-49.
26. Jiang, H.; Myshakin, E. M.; Jordan, K. D.; Warzinski, R. P., Molecular Dynamics Simulations of the Thermal Conductivity of Methane Hydrate. *J Phys Chem B* **2008**, *112*, 10207-10216.
27. Ikeda, T.; Mae, S.; Yamamuro, O.; Matsuo, T.; Ikeda, S.; Ibberson, R. M., Distortion of Host Lattice in Clathrate Hydrate as a Function of Guest Molecule and Temperature. *J Phys Chem A* **2000**, *104*, 10623-10630.
28. Murayama, K.; Takeya, S.; Alavi, S.; Ohmura, R., Anisotropic Lattice Expansion of Structure H Clathrate Hydrates Induced by Help Guest: Experiments and Molecular Dynamics Simulations. *J Phys Chem C* **2014**, *118*, 21323-21330.
29. Takeya, S., et al., Lattice Expansion of Clathrate Hydrates of Methane Mixtures and Natural Gas. *Angew Chem Int Edit* **2005**, *44*, 6928-6931.
30. Takeya, S., et al., Structure and Thermal Expansion of Natural Gas Clathrate Hydrates. *Chem Eng Sci* **2006**, *61*, 2670-2674.
31. Udachin, K. A.; Ratcliffe, C. I.; Ripmeester, J. A., Structure, Composition, and Thermal Expansion of Co2 Hydrate from Single Crystal X-Ray Diffraction Measurements. *J Phys Chem B* **2001**, *105*, 4200-4204.
32. Park, Y.; Choi, Y. N.; Yeon, S. H.; Lee, H., Thermal Expansivity of Tetrahydrofuran Clathrate Hydrate with Diatomic Guest Molecules. *J Phys Chem B* **2008**, *112*, 6897-6899.
33. Klapproth, A.; Goreshnik, E.; Staykova, D.; Klein, H.; Kuhs, W. F., Structural Studies of Gas Hydrates. *Can J Phys* **2003**, *81*, 503-518.
34. Chazallon, B.; Kuhs, W. F., In Situ Structural Properties of N-2-, O-2-, and Air-Clathrates by Neutron Diffraction. *J Chem Phys* **2002**, *117*, 308-320.
35. Kuhs, W. F.; Chazallon, B.; Radaelli, P. G.; Pauer, F., Cage Occupancy and Compressibility of Deuterated N-2-Clathrate Hydrate by Neutron Diffraction. *J Inclus Phenom Mol* **1997**, *29*, 65-77.
36. Manakov, A. Y.; Likhacheva, A. Y.; Potemkin, V. A.; Ogienko, A. G.; Kurnosov, A. V.; Ancharov, A. I., Compressibility of Gas Hydrates. *Chemphyschem* **2011**, *12*, 2475-2483.
37. Handa, Y. P., Compositions, Enthalpies of Dissociation, and Heat-Capacities in the Range 85-K to 270-K for Clathrate Hydrates of Methane, Ethane, and Propane, and Enthalpy of Dissociation of Isobutane Hydrate, as Determined by a Heat-Flow Calorimeter. *J Chem Thermodyn* **1986**, *18*, 915-921.
38. Rueff, R. M.; Sloan, E. D.; Yesavage, V. F., Heat-Capacity and Heat of Dissociation of Methane Hydrates. *Aiche J* **1988**, *34*, 1468-1476.
39. Leaist, D. G.; Murray, J. J.; Post, M. L.; Davidson, D. W., Enthalpies of Decomposition and Heat-Capacities of Ethylene-Oxide and Tetrahydrofuran Hydrates. *J Phys Chem-Us* **1982**, *86*, 4175-4178.
40. Ning, F. L.; Glavatskiy, K.; Ji, Z.; Kjelstrup, S.; Vlugt, T. J. H., Compressibility, Thermal Expansion Coefficient and Heat Capacity of Ch4 and Co2 Hydrate Mixtures Using Molecular Dynamics Simulations. *Phys Chem Chem Phys* **2015**, *17*, 2869-2883.
41. Barnes, B. C.; Sum, A. K., Advances in Molecular Simulations of Clathrate Hydrates. *Curr Opin Chem Eng* **2013**, *2*, 184-190.
42. Jendi, Z. M.; Servio, P.; Rey, A. D., Ab Initio Modelling of Methane Hydrate Thermodynamic Properties. *Phys Chem Chem Phys* **2016**, *18*, 10320-10328.

43. Costandy, J.; Michalis, V. K.; Tsimpanogiannis, I. N.; Stubos, A. K.; Economou, I. G., Lattice Constants of Pure Methane and Carbon Dioxide Hydrates at Low Temperatures. Implementing Quantum Corrections to Classical Molecular Dynamics Studies. *J Chem Phys* **2016**, *144*.
44. Costandy, J.; Michalis, V. K.; Tsimpanogiannis, I. N.; Stubos, A. K.; Economou, I. G., Molecular Dynamics Simulations of Pure Methane and Carbon Dioxide Hydrates: Lattice Constants and Derivative Properties. *Mol Phys* **2016**, *114*, 2672-2687.
45. Erfan-Niya, H.; Modarress, H.; Zaminpayma, E., Computational Study on the Structure Ii Clathrate Hydrate of Methane and Large Guest Molecules. *J Incl Phenom Macro* **2011**, *70*, 227-239.
46. Vlasic, T. M.; Servio, P.; Rey, A. D., Atomistic Modeling of Structure Ii Gas Hydrate Mechanics: Compressibility and Equations of State. *Aip Adv* **2016**, *6*.
47. Seol, J.; Lee, H., Natural Gas Hydrate as a Potential Energy Resource: From Occurrence to Production. *Korean J Chem Eng* **2013**, *30*, 771-786.
48. Brooks, J. M.; Kennicutt, M. C.; Fay, R. R.; Mcdonald, T. J.; Sassen, R., Thermogenic Gas Hydrates in the Gulf of Mexico. *Science* **1984**, *225*, 409-411.
49. Davidson, D. W.; Garg, S. K.; Gough, S. R.; Handa, Y. P.; Ratcliffe, C. I.; Ripmeester, J. A.; Tse, J. S.; Lawson, W. F., Laboratory Analysis of a Naturally-Occurring Gas Hydrate from Sediment of the Gulf of Mexico. *Geochim Cosmochim Ac* **1986**, *50*, 619-623.
50. Mak, T. C. W.; Mcmullan, R. K., Polyhedral Clathrate Hydrates. X. Structure of the Double Hydrate of Tetrahydrofuran and Hydrogen Sulfide. *J Chem Phys* **1965**, *42*, 2732-2737.
51. Kang, S. P.; Lee, H., Recovery of Co2 from Flue Gas Using Gas Hydrate: Thermodynamic Verification through Phase Equilibrium Measurements. *Environ Sci Technol* **2000**, *34*, 4397-4400.
52. Larsen, R.; Knight, C. A.; Sloan, E. D., Clathrate Hydrate Growth and Inhibition. *Fluid Phase Equilibr* **1998**, *150*, 353-360.
53. Sloan, E. D., Gas Hydrates: Review of Physical/Chemical Properties. *Energ Fuel* **1998**, *12*, 191-196.
54. Alavi, S.; Susilo, R.; Ripmeester, J. A., Linking Microscopic Guest Properties to Macroscopic Observables in Clathrate Hydrates: Guest-Host Hydrogen Bonding. *J Chem Phys* **2009**, *130*.
55. Alavi, S.; Ripmeester, J. A., Effect of Small Cage Guests on Hydrogen Bonding of Tetrahydrofuran in Binary Structure Ii Clathrate Hydrates. *J Chem Phys* **2012**, *137*.
56. Wooldridge, P. J.; Richardson, H. H.; Devlin, J. P., Mobile Bjerrum Defects - a Criterion for Ice-Like Crystal-Growth. *J Chem Phys* **1987**, *87*, 4126-4131.
57. Monreal, I. A.; Devlin, J. P.; Maslakci, Z.; Cicek, M. B.; Uras-Aytemiz, N., Controlling Nonclassical Content of Clathrate Hydrates through the Choice of Molecular Guests and Temperature. *J Phys Chem A* **2011**, *115*, 5822-5832.
58. Monreal, I. A.; Cwiklik, L.; Jagoda-Cwiklik, B.; Devlin, J. P., Classical to Nonclassical Transition of Ether-Hcn Clathrate Hydrates at Low Temperature. *J Phys Chem Lett* **2010**, *1*, 290-294.
59. Larionov, E. G.; Manakov, A. Y.; Zhurko, F. V.; Dyadin, Y. A., Cs-Ii Binary Clathrate Hydrates at Pressures of up to 15 Kbar. *J Struct Chem+* **2000**, *41*, 476-482.
60. Ripmeester, J. A.; Ratcliffe, C. I., Xe-129 Nmr-Studies of Clathrate Hydrates - New Guests for Structure-Ii and Structure-H. *J Phys Chem-Us* **1990**, *94*, 8773-8776.
61. Hess, B.; Kutzner, C.; van der Spoel, D.; Lindahl, E., Gromacs 4: Algorithms for Highly Efficient, Load-Balanced, and Scalable Molecular Simulation. *J Chem Theory Comput* **2008**, *4*, 435-447.
62. Takeuchi, F.; Hiratsuka, M.; Ohmura, R.; Alavi, S.; Sum, A. K.; Yasuoka, K., Water Proton Configurations in Structures I, Ii, and H Clathrate Hydrate Unit Cells. *J Chem Phys* **2013**, *138*.
63. Jorgensen, W. L.; Maxwell, D. S.; TiradoRives, J., Development and Testing of the Opls All-Atom Force

Field on Conformational Energetics and Properties of Organic Liquids. *J Am Chem Soc* **1996**, *118*, 11225-11236.
64. Potoff, J. J.; Siepmann, J. I., Vapor-Liquid Equilibria of Mixtures Containing Alkanes, Carbon Dioxide, and Nitrogen. *Aiche J* **2001**, *47*, 1676-1682.
65. Keasler, S. J.; Charan, S. M.; Wick, C. D.; Economou, I. G.; Siepmann, J. I., Transferable Potentials for Phase Equilibria-United Atom Description of Five- and Six-Membered Cyclic Alkanes and Ethers. *J Phys Chem B* **2012**, *116*, 11234-11246.
66. Abascal, J. L. F.; Vega, C., A General Purpose Model for the Condensed Phases of Water: Tip4p/2005. *J Chem Phys* **2005**, *123*.
67. Essmann, U.; Perera, L.; Berkowitz, M. L.; Darden, T.; Lee, H.; Pedersen, L. G., A Smooth Particle Mesh Ewald Method. *J Chem Phys* **1995**, *103*, 8577-8593.
68. Ratner, M. A., Understanding Molecular Simulation: From Algorithms to Applications, by Daan Frenkel and Berend Smit. *Physics Today* **1997**, *50*, 66.
69. Bussi, G.; Donadio, D.; Parrinello, M., Canonical Sampling through Velocity Rescaling. *J Chem Phys* **2007**, *126*.
70. Parrinello, M., Polymorphic Transitions in Single Crystals: A New Molecular Dynamics Method. *J Appl Phys* **1981**, *52*, 7182-7190.
71. Sun, J. X.; Zhang, L.; Ning, F. L.; Lei, H. W.; Liu, T. L.; Hu, G. W.; Lu, H. L.; Lu, J.; Liu, C. L.; Jiang, G. S.; Liang, J. Q.; Wu., N. Y. Production Potential and Stability of Hydrate-bearing Sediments at the Site 2 GMGS3-W19 in the South China Sea: A Preliminary Feasibility Study. *J Nat Gas Sci Eng*, in press. DOI: 10.1016/j.marpetgeo.2017.05.037
72. McBride, C.; Vega, C.; Noya, E. G.; Ramirez, R.; Sese, L. M., Quantum Contributions in the Ice Phases: The Path to a New Empirical Model for Water-Tip4pq/2005. *J Chem Phys* **2009**, *131*.
73. Conde, M. M.; Vega, C.; McBride, C.; Noya, E. G.; Ramirez, R.; Sese, L. M., Can Gas Hydrate Structures Be Described Using Classical Simulations? *J Chem Phys* **2010**, *132*.
74. J, T. D. In *Computer Simulation of Liquids*, 1989; pp 99-99.
75. Tse, J. S., Thermal Expansion of the Clathrate Hydrates of Ethylene Oxide and Tetrahydrofuran. *Le Journal De Physique Colloques* **1987**, *48*, 543-549.
76. Rawn, C. J.; Rondinone, A. J.; Chakoumakos, B. C.; Circone, S.; Stern, L. A.; Kirby, S. H.; Ishii, Y., Neutron Powder Diffraction Studies as a Function of Temperature of Structure Ii Hydrate Formed from Propane. *Can J Phys* **2003**, *81*, 431-438.
77. Senda, N.;: Winmostar, version 3.33 (URL http://winmostar.com/) .
78. Alavi, S.; Takeya, S.; Ohmura, R.; Woo, T. K.; Ripmeester, J. A., Hydrogen-Bonding Alcohol-Water Interactions in Binary Ethanol, 1-Propanol, and 2-Propanol + Methane Structure Ii Clathrate Hydrates. *J Chem Phys* **2010**, *133*.
79. Buch, V.; Devlin, J. P.; Monreal, I. A.; Jagoda-Cwiklik, B.; Uras-Aytemiz, N.; Cwiklik, L., Clathrate Hydrates with Hydrogen-Bonding Guests. *Phys Chem Chem Phys* **2009**, *11*, 10245-10265.
80. Koga, K.; Tanaka, H.; Nakanishi, K., Rearrangement of the Hydrogen-Bonded Network of the Clathrate Hydrates Encaging Polar Guest. *Mol Simulat* **1996**, *16*, 151-165.
81. Koga, K.; Tanaka, H.; Nakanishi, K., On the Stability of Clathrate Hydrates Encaging Polar Guest Molecules - Contrast in the Hydrogen-Bonds of Methylamine and Methanol Hydrates. *Mol Simulat* **1994**, *12*, 241-&.
82. Helgerud, M. B.; Waite, W. F.; Kirby, S. H.; Nur, A., Measured Temperature and Pressure Dependence of V-P and V-S in Compacted, Polycrystalline Si Methane and Sii Methane-Ethane Hydrate. *Can J Phys* **2003**,

81, 47-53.
83. Sloan, E. D., *Clathrate Hydrates of Natural Gas*; M. Dekker, 1998.
84. Yamamuro, O.; Oguni, M.; Matsuo, T.; Suga, H., Calorimetric Study of Pure and Koh-Doped Tetrahydrofuran Clathrate Hydrate†. *Journal of Physics & Chemistry of Solids* **1988**, *49*, 425-434.
85. Tombari, E.; Presto, S.; Salvetti, G.; Johari, G. P., Heat Capacity of Tetrahydrofuran Clathrate Hydrate and of Its Components, and the Clathrate Formation from Supercooled Melt. *J Chem Phys* **2006**, *124*.
86. Handa, Y. P.; Hawkins, R. E.; Murray, J. J., Calibration and Testing of a Tian-Calvet Heat-Flow Calorimeter Enthalpies of Fusion and Heat Capacities for Ice and Tetrahydrofuran Hydrate in the Range 85 to 270 K ☆. *J Chem Thermodyn* **1984**, *16*, 623-632.
87. Sengupta, S.; Guo, J.; Janda, K. C.; Martin, R. W., Exploring Dynamics and Cage-Guest Interactions in Clathrate Hydrates Using Solid-State Nmr. *J Phys Chem B* **2015**, *119*, 15485-15492.
88. Lehmkuhler, F., et al., Anomalous Energetics in Tetrahydrofuran Clathrate Hydrate Revealed by X-Ray Compton Scattering. *J Phys Chem Lett* **2010**, *1*, 2832-2836.
89. Stern, L. A.; Kirby, S. H.; Durham, W. B., Polycrystalline Methane Hydrate: Synthesis from Superheated Ice, and Low-Temperature Mechanical Properties. *Energ Fuel* **1998**, *12*, 201-211.
90. Staykova, D. K.; Kuhs, W. F.; Salamatin, A. N.; Hansen, T., Formation of Porous Gas Hydrates from Ice Powders: Diffraction Experiments and Multistage Model. *J Phys Chem B* **2003**, *107*, 10299-10311.
91. Kuhs, W. F.; Klapproth, A.; Gotthardt, F.; Techmer, K.; Heinrichs, T., The Formation of Meso- and Macroporous Gas Hydrates. *Geophys Res Lett* **2000**, *27*, 2929-2932.
92. Kuhs, W. F.; Genov, G.; Goreshnik, E.; Zeller, A.; Techmer, K. S.; Bohrmann, G., The Impact of Porous Microstructures of Gas Hydrates on Their Macroscopic Properties. *Int J Offshore Polar* **2004**, *14*, 305-309.
93. Durham, W. B.; Kirby, S. H.; Stern, L. A.; Zhang, W., The Strength and Rheology of Methane Clathrate Hydrate (Vol 108, Pg 2182, 2003). *J Geophys Res-Sol Ea* **2003**, *108*.
94. Jr, E. D. S.; Koh, C. A., Clathrate Hydrates of Natural Gases. *Crc Press* **2008**.